Self-assembly of quantum dots in a thin epitaxial film wetting an elastic substrate

M. S. Levine, A. A. Golovin, and S. H. Davis
Department of Engineering Sciences and Applied Mathematics, Northwestern University, Evanston, Illinois 60208-3100, USA

P. W. Voorhees
Department of Materials Sciences, Northwestern University, Evanston, Illinois 60208-3100, USA
(Received 7 January 2007; published 9 May 2007)

The evolution of quantum dots (QDs), resulting from the Asaro-Tiller-Grinfeld instability of an epitaxially strained thin solid film deposited on a solid elastic substrate, is considered. For a film that wets the substrate, a nonlocal integro-differential equation is derived that describes the evolution of QDs in the long-wave limit. The contribution of a *wetting stress*, that accounts for the change in wetting energy due to variation of the film thickness caused by the film deformation, is included. It is found that wetting interactions can damp the long-wave perturbations and lead to Turing-type instability. By means of a weakly nonlinear analysis, general conditions for the wetting potential are found for which the formation of spatially periodic arrays of QDs is possible. It is shown that in either the case of a two-layer or a glued-layer wetting potential, the spatially regular arrays of QDs are unstable. The numerical simulations show that the QD's evolution exhibits a power-law coarsening, with different characteristics giving different exponents.

DOI: 10.1103/PhysRevB.75.205312 PACS number(s): 68.65.Hb

I. INTRODUCTION

The formation of quantum dots (QDs) on surfaces of epitaxially strained thin solid films has attracted much attention in recent years due to the unique electronic properties of QDs and their important applications in optoelectronic devices[1–4] and bionanotechnology.[5] An important feature of QDs is that they can self-assemble; that is, they can form spontaneously as a result of an instability, thus providing an efficient and inexpensive method for their fabrication.

The principal mechanism leading to the formation of QDs in epitaxial films is associated with epitaxial stress that occurs in the film due to lattice mismatch between the film and the substrate. The elastic energy that accumulates in the film can be lowered by reconstruction of the film surface through surface undulations. This results in Asaro-Tiller-Grinfeld (ATG) instability,[6] leading to the formation of nanoscale surface structures (islands), QDs.[7–10]

The characteristic feature of the ATG instability is that all perturbations whose wavelengths are larger than a certain critical cutoff value are unstable (*long-wave* instability). The nonlinear evolution of this type of instability results in a coarsening of the surface structures, with larger islands growing at the expense of smaller ones, as observed in experiments.[11,12] However, in some experiments, the formation of stable arrays of equal-sized QDs has been observed[13] and the self-organization of spatially ordered QD arrays in multilayer structures has been demonstrated.[14] Since self-assembly of spatially regular arrays of QDs is desirable in several optoelectronic applications,[4] investigation of the conditions under which the coarsening can cease and regular QD arrays can form is important.

The theoretical investigation of self-assembly and evolution of QDs in thin epitaxial films has received a great deal of attention. In Ref. 15, the formation and coarsening of QDs caused by the ATG instability mechanism were investigated by numerically solving a nonlinear evolution equation for the film surface shape and the resulting coarsening kinetics was in accord with experimental observations.[12] A theoretical analysis of the stability of a hexagonal array of cones on the surface of an elastically strained solid was performed in Ref. 16. It was shown that elastic interactions between the cones can lead to array metastability. Elastic interactions can also stabilize spatially regular QD arrays in multilayer structures[17]; however, other stabilization mechanisms are also possible.[18] Numerical simulations of the self-assembly of regular QD arrays in multilayer structures were performed in Ref. 19.

Another physical mechanism that can cause the spatial ordering of QDs in thin epitaxial films is associated with wetting interactions between the film and the substrate. As was shown in Refs. 20–22, wetting interactions can stabilize long-wave perturbation modes and change the spectrum of the ATG instability from long-wave type to Turing (short-wave) type, with the instability threshold corresponding to a particular finite wavelength. Turing instability is known to result in the formation of spatially regular patterns.[23]

An analysis of the pattern formation in a thin epitaxial film caused by the interplay between elastic and wetting interactions was performed in Ref. 21 for the case of a rigid substrate in the long-wave limit; the possibility of the formation of stable, spatially regular arrays of QDs was demonstrated analytically and numerically. In Ref. 24 it was also shown that, in the presence of a strong surface-energy anisotropy, self-organization of regular QD arrays is possible even without epitaxial stress, solely as a result of the coupling between wetting interactions and a thermodynamic faceting instability. A combined effect of elastic stress, surface-energy anisotropy, and wetting interactions on the formation of QDs in a thin epitaxial film was investigated in Refs. 25 and 26. Numerical simulations performed for 1+1 (Ref. 26) and 2+1 (Ref. 25) interfaces showed self-assembly of spatially periodic arrays of faceted pyramids.

Another important factor that affects the formation of QDs in epitaxial films is the elastic properties of the substrate. The substrate elasticity results in a nonanalytic spectrum of the ATG instability[8,10] and can substantially affect the nonlinear dynamics of QD formation. The effect of the

substrate elasticity on the self-assembly of QDs in the presence of wetting interactions was studied in Ref. 27. A nonlocal, integro-differential equation describing the evolution of the film surface was derived in the long-wave limit, and the formation of a single localized island was investigated (see also Ref. 28). This analysis has recently been generalized in Ref. 29 to include certain nonlinear elastic effects. It was claimed that the combined effect of nonlinear stress and wetting can terminate the coarsening process and lead to the formation of irregular arrays of equal-sized islands. Phase-field numerical simulations of island formation in the presence of wetting effects and elastic interaction between the film and the substrate were performed in Refs. 30 and 31.

Despite the large number of theoretical investigations of self-assembly of QDs in thin solid films, the question as to the conditions under which the QD coarsening ceases and a spatially regular array of QDs can form still remains open. Specifically, the fact that ordered QD arrays have not been observed in experiments on the instability of thin epitaxial films needs to be understood. This problem can be approached by means of a weakly nonlinear stability analysis near the ATG instability threshold that would allow one to understand the nature of the bifurcation of a regular pattern from a homogeneous state. Also, it can be shown that wetting interactions between the film and the substrate yield an additional normal stress at the film free surface that can be called a *wetting stress*. This stress originates from the dependence of the wetting potential on the film thickness.

In this paper, we investigate the formation of quantum dots driven by ATG instability and wetting interactions between the film and the substrate, accounting for the substrate elasticity and wetting stress. We perform linear and weakly nonlinear analyses in order to determine the possibility of the formation of spatially regular QD arrays. We show that, in the case of two-layer and glued-layer wetting potentials, such arrays result from a subcritical bifurcation and are therefore unstable. We also perform numerical simulations of a nonlocal integro-differential equation describing the surface evolution in the long-wave approximation and determine the coarsening kinetics.

II. PROBLEM STATEMENT

Consider an epitaxially strained thin solid film that wets a solid, semi-infinite elastic substrate. The film surface $z=h(\mathbf{x},t)$ evolves due to surface diffusion, described by[10]

$$\frac{\partial h}{\partial t} = \mathcal{D}(1+|\nabla h|^2)^{1/2}\nabla_S^2[\mathcal{E}(h) - 2\gamma\mathcal{K} + \mathcal{W}(h)], \qquad (1)$$

where z is the coordinate normal to the substrate, $\mathbf{x}=(x,y)$ are the coordinates in the plane parallel to the planar substrate-film interface, ∇_S^2 is the surface Laplacian, $\mathcal{E}(h)$ is part of the surface chemical potential related to the elastic energy in the film which is determined by the solution of the corresponding elastic problem (see below), $\mathcal{W}(h)$ is part of the surface chemical potential due to wetting interactions with the substrate (wetting potential), γ is the surface free energy, assumed to be isotropic—i.e., independent of the surface orientation—and $2\mathcal{K}=[(1+h_x^2)h_{yy}+(1+h_y^2)h_{xx}-2h_xh_yh_{xy}]/(1+|\nabla h|^2)^{3/2}$ is the mean surface curvature; $\mathcal{D}=D_SS_0\Omega V_0/k_B\theta$, where D_S is the surface mobility of atoms, S_0 is the number of atoms per unit area of the surface, k_B is the Boltzmann constant, θ is the absolute temperature, Ω is the atomic volume, and V_0 is the atomic volume of lattice sites on the film surface.

We consider two models for the wetting interactions (see also Ref. 24): the two-layer and glued-layer models. In a *two-layer wetting model*, the surface energy depends on the film thickness according to[33–35]

$$\gamma(h) = \gamma_f + (\gamma_s - \gamma_f)e^{-h/\delta_w}, \qquad (2)$$

where γ_s is the surface energy of the substrate in the absence of the film, γ_f is the energy of the film free surface far from the substrate, and δ_w is the characteristic wetting length. In this case, the wetting potential is[34]

$$\mathcal{W} = (d\gamma/dh)/\sqrt{1+|\nabla h|^2}. \qquad (3)$$

In a *glued-layer wetting model*, the wetting potential has a singularity for $h\to 0$ and exponentially decays for $h\to\infty$; we set

$$\mathcal{W} = -w(h/\delta_w)^{-\alpha_w}\exp(-h/\delta_w). \qquad (4)$$

Here $w>0$ characterizes the strength of the wetting interactions and $\alpha_w>0$ characterizes the singularity. This singularity is a simple phenomenological continuum model of a very large potential barrier for the removal of an ultrathin (possibly monolayer) wetting layer that persists between surface mounds during the Stranski-Krastanov growth process (see also Refs. 36–38).

We choose a coordinate system such that $z<0$ corresponds to the semi-infinite substrate, and $0<z<h(\mathbf{x},t)$ corresponds to the film. We assume that mechanical equilibrium exists in the system at all times; therefore, $\partial_j\sigma_{ij}^{f,s}=0$, where σ_{ij} is the stress tensor expressed in terms of the strain tensor E_{ij}, ∂_j denotes partial differentiation with respect to the coordinate $j=1,2,3$ corresponding to the coordinates x,y,z, respectively, and the superscripts f and s refer to the film and the substrate, respectively. The stress and strain tensors are related by Hooke's law,[32]

$$\sigma_{ij} = 2\mu\left[\left(\frac{\nu}{1+\nu}\right)\delta_{ij}E_{kk} + E_{ij}\right], \quad E_{ij} = \frac{1}{2}(\partial_j u_i + \partial_i u_j), \qquad (5)$$

where u_i is the ith Cartesian coordinate of the displacement vector, $i=1,2,3$, μ is the elastic shear modulus, ν is the Poisson's ratio, δ_{ij} is Kronecker's delta, and the usual summation over repeated indices is assumed. Thus, the condition of mechanical equilibrium is described by the Navier equations in the film and in the substrate,[32]

$$(1-2\nu^{f,s})\partial_k^2 u_i^{f,s} + \partial_i\partial_k u_k^{f,s} = 0. \qquad (6)$$

The elastic energy in Eq. (1) is $\mathcal{E}(h)=\frac{1}{2}\sigma_{ij}E_{ij}|_{z=h}$.

In the presence of wetting interactions, the boundary conditions that describe the stress balance at the film free surface and at the film-substrate interface require special consider-

ation. In both wetting models, we assume that the wetting potential depends on the film thickness which can change by two mechanisms: (i) accumulation (or redistribution) of material at the free surface and (ii) deformation of the film. If, as a result of the film deformation, the local displacements of the film free surface and the film-substrate interface in the z direction are δh_f and δh_s, respectively, then the film thickness changes by $\delta h = \delta h_f - \delta h_s$, causing the film surface energy to change by $(d\gamma/dh)\delta h$. This means that additional stresses in the z direction, $\mp d\gamma/dh$, act on the film free surface and the film-substrate interface, respectively. The work of these stresses causes this energy change. Similarly, if wetting interactions between the film and the substrate are described by the glued-layer wetting potential given by Eq. (4), then the additional stresses acting on the film free surface and the film-substrate interface are $\mp h d\mathcal{W}/dh$, respectively. Thus, in the presence of wetting interactions, characterized by an additional wetting energy that depends on the local film thickness, one should include a *wetting stress* acting on the film free surface and on the film-substrate interface. This wetting stress accounts for the change of the film energy due to the variation of the film thickness caused by the film deformation, while the term $\mathcal{W}(h)$ in the surface diffusion equation (1) accounts for the change of the film energy when the film thickness changes due to the material redistribution. Note that this consideration is valid only in the long-wave approximation, when wetting interactions can be described by a function that depends on the local film thickness only.

In the following analysis, unless specified otherwise, we consider the two-layer wetting model. Thus, the stress balance boundary conditions at the film free surface and at the film-substrate interface read

$$\sigma_{ij}^f n_j + \frac{\partial \gamma}{\partial h}\delta_{i3} = 0 \quad \text{on } z = h(x,y,t), \tag{7}$$

$$\sigma_{ij}^f n_j - \sigma_{ij}^s n_j + \frac{\partial \gamma}{\partial h}\delta_{i3} = 0 \quad \text{on } z = 0, \tag{8}$$

where n_j is the unit normal to the film surface and $\partial\gamma/\partial h$ is the wetting stress.

At the film-substrate interface, continuity of displacement taking into account the lattice mismatch between the film and the substrate holds,

$$u_i^f = u_i^s + \epsilon \begin{bmatrix} x \\ y \\ 0 \end{bmatrix}. \tag{9}$$

Here, ϵ is the misfit strain in the film, defined by

$$\epsilon = \frac{a_s - a_f}{a_f}, \tag{10}$$

where a_f and a_s are the lattice spacings of the film and the substrate, respectively; $\epsilon > 0$ corresponds to tensile strain and $\epsilon < 0$ to the compressive strain. Finally, we require the strains in the substrate far away from the film to decay to zero,

$$E_{ij}^s \to 0 \quad \text{as } z \to -\infty. \tag{11}$$

III. STEADY-STATE SOLUTION

The governing equations in Sec. II describe the stress state and surface evolution of an epitaxially strained film. They have a basic-state solution corresponding to a completely relaxed, stress-free substrate,

$$\bar{u}_i^s = 0, \quad \bar{\sigma}_{ij}^s = 0 \quad \text{for } i,j = 1,2,3, \tag{12}$$

and a planar film with spatially uniform stress and strain,

$$\bar{u}_1^f = \epsilon x, \quad \bar{u}_2^f = \epsilon y, \quad \bar{u}_3^f = -\frac{1}{1-\nu_f}\left[2\epsilon\nu_f + \frac{1-2\nu_f}{2\mu_f}\frac{\partial\gamma}{\partial h}\right]z, \tag{13}$$

$$\bar{\sigma}_{11}^f = \bar{\sigma}_{22}^f = \frac{1}{1-\nu_f}\left[2\epsilon\mu_f(1+\nu_f) - \nu_f\frac{\partial\gamma}{\partial h}\right], \quad \bar{\sigma}_{33}^f = -\frac{\partial\gamma}{\partial h}. \tag{14}$$

Note that even in the absence of epitaxial strain, the wetting interactions with the substrate produce *wetting strain* and *wetting stress* in the film:

$$\bar{E}_{33}^w = -\frac{1-2\nu_f}{2\mu_f(1-\nu_f)}\frac{\partial\gamma}{\partial h}, \quad \bar{\sigma}_{11}^w = \bar{\sigma}_{22}^w = -\frac{\nu_f}{1-\nu_f}\frac{\partial\gamma}{\partial h},$$

$$\bar{\sigma}_{33}^w = -\frac{\partial\gamma}{\partial h}. \tag{15}$$

In the presence of epitaxial strain, wetting interactions modify the strain in the film as well as all components of the stress. It is interesting to note that the presence of wetting stress breaks the symmetry between compressive and tensile epitaxial strains. Indeed, as follows from Eq. (13), when the epitaxial strain is compressive ($\epsilon < 0$), the corresponding vertical strain has the same sign as the wetting strain and the two strains add to increase the total vertical strain. Alternatively, when the epitaxial strain is tensile ($\epsilon > 0$), the signs of the epitaxial and wetting strains in the vertical direction are opposite which decreases the total vertical strain. The total elastic energy stored in the film due to epitaxial and wetting stresses, however, is independent of the sign of ϵ and $\partial\gamma/\partial h$:

$$\mathcal{E}_0 = \frac{1}{2}\bar{\sigma}_{ij}^f\bar{E}_{ij}^f = 2\epsilon^2\mu_f\frac{1+\nu_f}{1-\nu_f} + \frac{1}{2\mu_f}\frac{1-2\nu_f}{1-\nu_f}\left(\frac{\partial\gamma}{\partial h}\right)^2. \tag{16}$$

In the next section we perform a linear stability analysis of this basic state of an epitaxial film in the presence of epitaxial and wetting stresses.

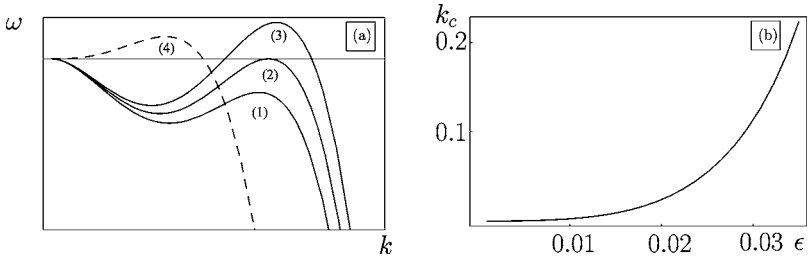

FIG. 1. (a) Sketch of dispersion curves defined by Eq. (18) for (1) $B^2/(4AC)<1$, (2) $B^2/(4AC)=1$, (3) $B^2/(4AC)>1$, and (4) $A=0$. (b) Critical wave number k_c as a function of the epitaxial strain for the two-layer wetting potential with parameters typical of a Ge on Si system (cgs units): $\mu_f=10^{12}$, $\mu_0=0.8$, $\gamma_f=2\times10^3$, $\Delta\gamma=2\times10^2$, $\nu_f=0.198$, and $\nu_s=0.217$.

IV. LINEAR STABILITY ANALYSIS

In this section, we study the stability of a planar film in the basic state described by Eqs. (12)–(14). The film dynamics is governed by Eqs. (1) and (6)–(11). We consider infinitesimal perturbations of the planar film, $h=\bar{h}+\hat{h}e^{\omega t+i\mathbf{k}\cdot\mathbf{x}}$, and the displacement vectors

$$\mathbf{u}^{f,s}=\mathbf{u}_0^{f,s}+\hat{\mathbf{f}}^{f,s}(z)e^{\omega t+i\mathbf{k}\cdot\mathbf{x}}, \tag{17}$$

and linearize the problem (1)–(11). The solvability condition for the linear problem gives the dispersion relation between the perturbation growth rate ω and the wave vector $\mathbf{k}$. In the long-wave approximation—i.e., for $2\pi/k\gg\bar{h}$—this dispersion relation reads

$$\mathcal{D}^{-1}\omega=-Ak^2+Bk^3-Ck^4, \tag{18}$$

where $k=|\mathbf{k}|$ and

$$A=\left[1+\frac{\beta_f}{\mu_f\alpha_f}\gamma'(\bar{h})\right]\gamma'(\bar{h}), \tag{19}$$

$$B=4\frac{\alpha_s}{\alpha_f^2}\mu_0(1+\nu_f)\{2\epsilon^2(1+\nu_f)\mu_s-\epsilon\nu_f[\gamma'(\bar{h})+\bar{h}\gamma''(\bar{h})]\}, \tag{20}$$

$$C=\gamma+\frac{2\bar{h}}{\alpha_f^3}(1+\nu_f)\{\epsilon[4\nu_f\gamma'(\bar{h})C_1+\bar{h}\gamma''(\bar{h})C_2]-8\epsilon^2\mu_s(1+\nu_f)(C_1-\alpha_f)\}, \tag{21}$$

where

$$\alpha_{f,s}=2(1-\nu_{f,s}),\quad \beta_{f,s}=1-2\nu_{f,s},\quad \mu_0=\mu_f/\mu_s,$$

$$C_1=\alpha_f+\alpha_f\beta_s\mu_0-\alpha_s^2\mu_0^2,\quad C_2=4\alpha_f+3\alpha_f\beta_s\mu_0-4\alpha_s^2\mu_0^2. \tag{22}$$

In the absence of wetting, $\gamma'(\bar{h})=\gamma''(\bar{h})=0$ and $A=0$ Eq. (18) reduces to the long-wave limit of the dispersion relation obtained in Ref. 10. [Note that for $\gamma'(\bar{h})=\gamma''(\bar{h})=0$ the long-wave expansion (18) is valid for $\bar{h}\mu_f\epsilon^2\ll\gamma$. For typical values of $\bar{h}=1$ nm, $\mu_s=10^{12}$ erg/cm^3, $\gamma=2\times10^3$ erg/cm^2, and $\epsilon=0.03$ one obtains $\bar{h}\mu_f\epsilon^2/\gamma=0.05\ll1$.]

When wetting interactions between the film and the substrate are present, $\gamma'(\bar{h})<0$, $\gamma''(\bar{h})>0$, and the dispersion relation contains an additional term $-Ak^2$, which becomes dominant for small wave numbers. Had the *wetting stress* not been accounted for, one would have obtained $A=\gamma'(\bar{h})>0$ which would mean that the wetting interactions always damp long-wave modes. However, this is not always so if the *wetting stress* is taken into account. In this case, the long-wave modes are damped ($A>0$) only if $|\gamma'(\bar{h})|<\mu_f\alpha_f/\beta_f\approx2\mu_f$; otherwise, the long-wave modes are *destabilized* by wetting stress. This destabilization is even stronger than that produced by the epitaxial stress; indeed, in this case the growth rate is proportional to k^2, rather than to k^3, in the absence of wetting.

This change-of-sign effect, however, is probably not relevant to common semiconductor materials, such as Ge or Si. Indeed, taking $\mu_f=10^{12}$ erg/cm^3, $\gamma_s-\gamma_f\equiv\Delta\gamma=2\times10^2$ erg/cm^2, $\delta_w=1$ nm, and $\bar{h}=1$ nm, one obtains $\gamma'(\bar{h})\approx10^9$ erg/cm^3 (which is in accordance with *ab initio* calculations performed in Ref. 35) and $\gamma'(\bar{h})\ll\mu_f$. Thus, in this case $A>0$ and the long-wave modes are always damped by the wetting interactions.

Typical dispersion curves for the case when wetting interactions damp the long-wave modes are schematically shown in Fig. 1(a). The film becomes unstable for $B^2-4AC>0$. One can see that this damping changes the instability spectrum from long-wave (spinodal decomposition) type to short-wave (Turing) type, thus leading to the possibility of changing the system evolution from Ostwald ripening to the formation of stable spatially periodic patterns. Figure 1(b) shows the wave number $k_c=B/2C$, corresponding to the most rapidly growing mode, as a function of the lattice mismatch ϵ for typical values of the parameters: $\mu_0=0.8$, $\gamma_f=2\times10^3$ (erg/cm^2), $\Delta\gamma=2\times10^2$ (erg/cm^2), $\nu_f=0.198$, and $\nu_s=0.217$. One can see that the long-wave approximation is appropriate here.

Another interesting effect of wetting stress is associated with the sign of the coefficient B in the dispersion relation (18). In the absence of wetting interactions, $B\sim\mu_f\epsilon^2>0$ which describes the destabilization effect of the epitaxial stress. The presence of wetting stress can change the sign of this coefficient. Indeed, $\gamma'(\bar{h})+\bar{h}\gamma''(\bar{h})=(\Delta\gamma/\delta_w)e^{-\bar{h}/\delta_w}(\bar{h}/\delta_w-1)\equiv\bar{\gamma}'(\bar{h})>0$ for $\bar{h}>\delta_w$ and $\bar{\gamma}'(\bar{h})<0$ for $\bar{h}<\delta_w$. In the case of a compressive epitaxial strain $\epsilon<0$, the coefficient B is positive for $\bar{\gamma}'(\bar{h})>2\epsilon\mu_s(1+\nu_f^{-1})$, and in the case of a tensile epitaxial strain $\epsilon>0$, the coefficient B is positive for $\bar{\gamma}'(\bar{h})<2\epsilon\mu_s(1+\nu_f^{-1})$. This also shows that the presence of the wetting stress *breaks the symmetry* between compressive and tensile epitaxial strains. This effect is more pronounced for *smaller* epitaxial strain.

The stability analysis described above is illustrated in Figs. 2–6. Figure 2 shows the neutral stability boundaries in

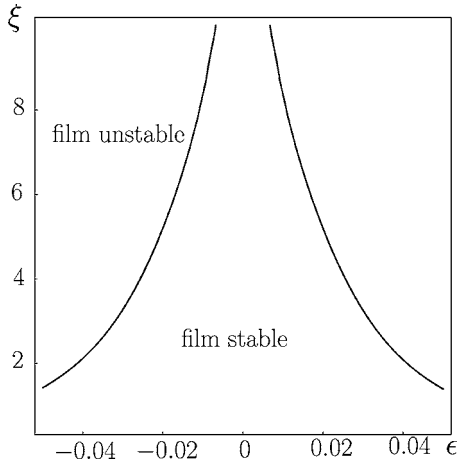

FIG. 2. Stability regions for a planar epitaxial film with two-layer wetting potential for parameters as in Fig. 1.

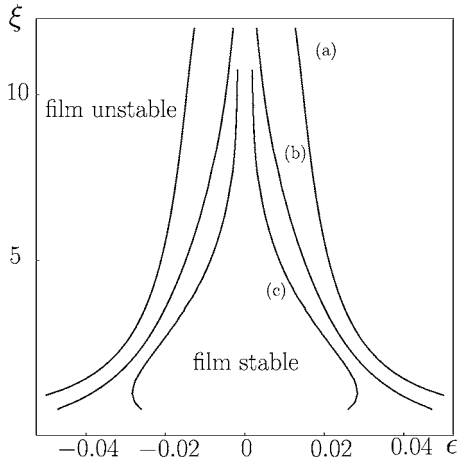

FIG. 4. Stability regions for a planar epitaxial film with a two-layer wetting potential for (a) $\mu_0=0.01$, (b) $\mu_0=0.50$, and (c) $\mu_0=10$. See Fig. 1 for other parameter values.

the (ϵ,ξ) parameter plane where $\xi=\bar{h}/\delta_w$. One can see that if the epitaxial strain is sufficiently large, then the film is always unstable. However, if the epitaxial strain is small enough, then the film becomes unstable only if its thickness exceeds a critical value, $\bar{h}>h_c(\epsilon)$. Figure 3 shows that for some intervals of the epitaxial strain and some parameter values there can be *two* critical values of the film thickness, h_c^+ and h_c^-, that bound the *interval* of the film stability. This corresponds to the boxed region in Fig. 3(a), enlarged in Fig. 3(b). Here, the film is unstable for $\bar{h}>h_c^+$ and $\bar{h}<h_c^-$. The film instability for smaller thickness can be explained by the destabilizing effect of the wetting stress which is more pronounced for smaller thicknesses due to exponential decay of wetting interactions.

Figure 4 shows how the neutral-stability boundaries change as the film stiffness (shear modulus) varies relative to that of the substrate, which is characterized by the parameter μ_0. One can see that the stability region narrows as the film's stiffness increases. Note that the interval of epitaxial strains where the film is stable for $h_c^-<\bar{h}<h_c^+$ exists only for sufficiently large μ_0.

Figure 5 shows how the neutral-stability boundaries change as the wetting strength varies, which is characterized by $\Delta\gamma=\gamma_s-\gamma_f$ in Eq. (2). One can see that as the wetting interactions become stronger, the film stability increases.

One can also see from Figs. 2–5 that for a film with a given thickness there exist two critical values of epitaxial strain (positive and negative for tensile and compressive strains, $\epsilon_c^{\pm}$, respectively) above which the film becomes unstable. Figure 6 shows these critical values of the epitaxial strain as functions of $\Delta\gamma$ and μ_0. In the left figure, one can see $\epsilon_c^{\pm}(\Delta\gamma)$ for $\mu_0=10.0$ and different film thickness. In the right figure, one can see $\epsilon_c^{\pm}(\mu_0)$ for $\Delta\gamma=2\times10^2$ erg/cm^2 and different thickness of the film. Note that $\epsilon_c^{\pm}$ tend to constant values with an increase of μ_0. Note also that the stability region for $\xi=1.0$ is larger than those for $\xi=0.0$ and $\xi=2.0$. This corresponds to the case shown in Fig. 3(b).

V. SURFACE EVOLUTION EQUATION IN LONG-WAVE APPROXIMATION

In this section, we derive an evolution equation for the shape of the film surface in the long-wave approximation using the general surface-diffusion equation (1). Here we follow closely the derivation presented in Ref. 27.

We introduce a small parameter $\alpha=\bar{h}/l\ll1$; rescale the variables $h\to\alpha lH$, $(x,y)\to l(x',y')$, $z\to\alpha lz'$, $t\to\pi t'$, and $u^f_{1,2,3}(x,y,z)\to lU^f_{1,2,3}(x',y',z')$; and consider the expansions $\sigma_{ij}=\sigma_{ij}^{(0)}+\alpha\sigma_{ij}^{(1)}+\alpha^2\sigma_{ij}^{(2)}+\cdots$, $E_{ij}=E_{ij}^{(0)}+\alpha E_{ij}^{(1)}+\alpha^2E_{ij}^{(2)}+\cdots$, and $\mathcal{E}=\mathcal{E}_0+\alpha\mathcal{E}_1+\alpha^2\mathcal{E}_2+\cdots$, where $\mathcal{E}_0=2\epsilon^2\mu_f(1+\nu_f)/(1-\nu_f)$. We also use the following scaling for the wetting stress: $\partial\gamma/\partial h=\alpha\mu_f\widetilde{\mathcal{W}}(H)$. We choose the time scale $\tau=l^4/(D\gamma_f)$,

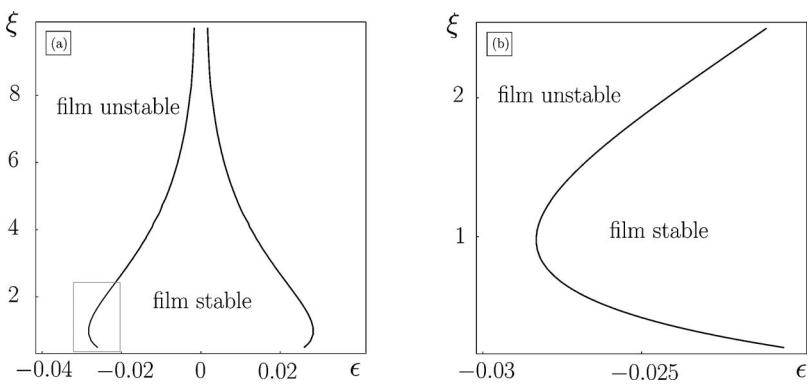

FIG. 3. (a) Stability regions for a planar epitaxial film with a two-layer wetting potential for $\mu_0=10$. See Fig. 1 for other parameter values. (b) Close-up of the boxed region in (a).

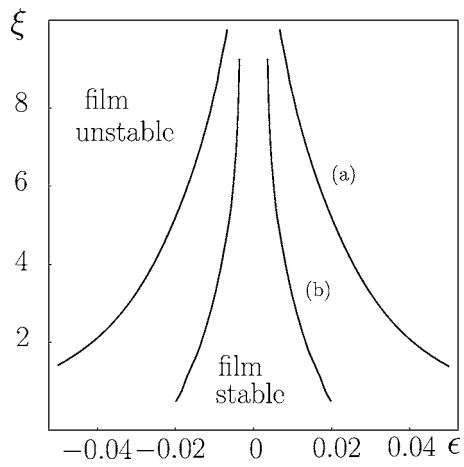

FIG. 5. Stability regions for a planar epitaxial film with a two-layer wetting potential (cgs units): (a) $\Delta\gamma=10^2$ and (b) $\Delta\gamma=1$. See Fig. 1 for other parameter values.

and the length scale $l=\gamma_f/\mathcal{E}_0$, and obtain from Eq. (1), in the order $O(\alpha)$, the following evolution equation in the long-wave approximation:

$$\frac{\partial H}{\partial t}=\nabla^2[\tilde{\mathcal{E}}_1-\nabla^2 H+\widetilde{W}], \tag{23}$$

where $\tilde{\mathcal{E}}_1=\mathcal{E}_1/\mathcal{E}_0$ and $\widetilde{W}=(\mu_f/\mathcal{E}_0)\widetilde{\mathcal{W}}$, and we omit primes in the rescaled coordinates.

We determine $\tilde{\mathcal{E}}_1$ by solving the elasticity problem. First, we find the solution of the elastic problem in the film and the substrate that satisfy the boundary conditions (7) and (8), respectively. We then use the boundary conditions (9) in order to solve for unknown coefficients of the elasticity problem solution in the film (see Ref. 27 for details). Finally, we obtain

$$\tilde{\mathcal{E}}_1=\frac{1}{4\pi^2}\int k\tilde{\mathcal{E}}_{1\mathbf{k}}e^{-i\mathbf{k}\cdot\mathbf{x}}d^2\mathbf{k},$$

$$\tilde{\mathcal{E}}_{1\mathbf{k}}=E_0\left(-H_{\mathbf{k}}+\frac{1}{2\epsilon}\frac{\nu_f}{1+\nu_f}(\widetilde{HW})_{\mathbf{k}}\right), \tag{24}$$

where $H_{\mathbf{k}}$ and $(\widetilde{HW})_{\mathbf{k}}$ are the respective Fourier transforms of H and $\widetilde{HW}$ and

$$E_0=\frac{2\mu_f(1+\nu_f)(1-\nu_s)}{\mu_s(1-\nu_f)}. \tag{25}$$

Equations (23) and (24) are a generalization of the long-wave equation obtained in Ref. 27 for the presence of wetting stress. However, as shown above, the effect of the wetting stress is negligible for typical semiconductor systems; thus, we omit the term $(\widetilde{HW})_{\mathbf{k}}$ in Eqs. (24) in the analysis that follows. After further rescaling, $t\to t/E_0^2$, $\mathbf{x}\to\mathbf{x}/E_0$, Eq. (23) has the following form:

$$\frac{\partial H}{\partial t}=\nabla^2[\mathcal{E}_1[H]-\nabla^2 H+W(H)], \tag{26}$$

where $W=\widetilde{W}/E_0^2$ and

$$\mathcal{E}_1[H]=\frac{1}{4\pi^2}\int kH_{\mathbf{k}}e^{-i\mathbf{k}\cdot\mathbf{x}}d^2\mathbf{k}. \tag{27}$$

VI. FORMATION OF SURFACE STRUCTURES: WEAKLY NONLINEAR ANALYSIS

In this section, we investigate the nonlinear evolution of surface structures near the short-wave instability threshold in order to determine if the formation of a spatially periodic array of dots is possible. We consider $H=H_0+\widetilde{H}, |\widetilde{H}|\ll H_0$ and expand

$$W(H)=w_0+w_1\widetilde{H}+w_2\widetilde{H}^2+w_3\widetilde{H}^3+\cdots. \tag{28}$$

Linearizing Eq. (26) for $\widetilde{H}\sim e^{\omega t+i\mathbf{k}\cdot\mathbf{x}}$, one obtains

$$\omega=-w_1k^2+k^3-k^4. \tag{29}$$

The onset of instability corresponds to $w_1=w_{1c}=1/4$ and $k=k_c=1/2$.

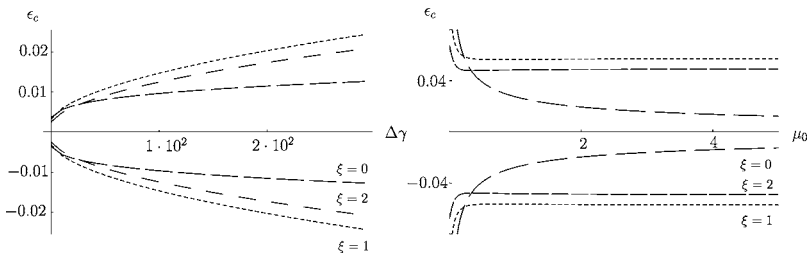

FIG. 6. Critical values $\epsilon_c^{\pm}$ as functions of $\Delta\gamma$ for $\mu_0=10.0$ (left) and μ_0 for $\Delta\gamma=2\times10^2$ (right) for different initial film thickness (for a two-layer wetting potential). Other parameter values correspond to those in Fig. 1 (cgs units).

Now we consider the weakly nonlinear case corresponding to $w_1=1/4-\varepsilon^2\sigma$, $\varepsilon \ll 1$. First consider quasi-one-dimensional structures (*wires*). We introduce the long scale coordinate $X=\varepsilon x$ and the slow time $T=\varepsilon^2 t$, and consider the expansions

$$\widetilde{H} = \varepsilon(H_1 + \varepsilon H_2 + \cdots), \tag{30}$$

$$\mathcal{E}_1 = \mathcal{E}_{10} + \varepsilon\mathcal{E}_{11} + \varepsilon^2\mathcal{E}_{12} + \cdots. \tag{31}$$

Here,

$$H_1 = \varepsilon[A(X,T)e^{ik_c x} + \text{c.c.}],$$

$$H_2 = \varepsilon^2[B(X,T) + A_2(X,T)e^{2ik_c x} + \text{c.c.}], \tag{32}$$

where $A(X,T)$ is the complex amplitude of the spatially periodic, unstable mode, and $B(X,T)$ is the real amplitude of the zero mode. The linear operator $\mathcal{E}_1$ acts on a Fourier mode $A(X,T)e^{ikx}$ as

$$\mathcal{E}_1[A(X,T)e^{ikx}] = [\mathcal{E}_{10}(k) + \varepsilon\mathcal{E}_{11}(k,\partial_X) + \varepsilon^2\mathcal{E}_{12}(k,\partial_X) + \cdots]A(X,T)e^{ikx}, \tag{33}$$

where

$$\mathcal{E}_{10}(k) = -|k|, \quad \mathcal{E}_{11}(k,\partial_X) = i\,\text{sgn}(k)\partial_X,$$

$$\mathcal{E}_{12}(k,\partial_X) = -\,\text{sgn}(k)\partial_{XX}. \tag{34}$$

Using these expansions, we obtain successive problems in orders of ε. At $O(\varepsilon^2)$, we find $A_2=-4w_2A^2$. Finally, the solvability conditions at $O(\varepsilon^3)$ and $O(\varepsilon^4)$ yield the system of coupled amplitude equations:

$$A_T = \frac{1}{4}\sigma A + \frac{1}{2}A_{XX} - \lambda|A|^2A + sAB,$$

$$B_T = \frac{1}{4}B_{XX} - 4s(|A|^2)_{XX}, \tag{35}$$

where

$$\lambda = \frac{3}{4}w_3 - 2w_2^2, \quad s = -\frac{1}{2}w_2. \tag{36}$$

The system of amplitude equations (35) has a stable, stationary solution $A=(\frac{\sigma}{4\lambda})^{1/2}$, $B=0$, corresponding to spatially periodic patterns if $\lambda > 16s^2$,[40,21]—i.e., if

$$w_3 > 8w_2^2. \tag{37}$$

Condition (37) defines a region in the parameter space in which one could observe the formation of stable, periodic array of wires. First consider a *glued-layer* wetting potential defined by Eq. (4). Translating (37) into physical parameters gives

$$\frac{e^{\xi}[\alpha^3+\xi^3+3\alpha^2(1+\xi)+\alpha(2+3\xi+3\xi^2)]\xi^{1+\alpha}}{12(\alpha+\alpha^2+2\alpha\xi+\xi^2)^2} > \frac{w\gamma_f}{\delta\mathcal{E}_0^2}. \tag{38}$$

and with the instability-onset condition $w_1=1/4$,

$$\frac{w\gamma_f}{\delta\mathcal{E}_0^2} = \frac{\xi^\alpha e^{-\xi}}{4}\left(1+\frac{\alpha}{\xi}\right)^{-1}, \tag{39}$$

yields

$$\frac{e^{\xi}[\alpha^3+\xi^3+3\alpha^2(1+\xi)+\alpha(2+3\xi+3\xi^2)]\xi^{1+\alpha}}{12(\alpha+\alpha^2+2\alpha\xi+\xi^2)^2} - \frac{\xi^\alpha e^{-\xi}}{4}\left(1+\frac{\alpha}{\xi}\right)^{-1} > 0. \tag{40}$$

Inequality (40) is satisfied only for $\xi \ll 1$—i.e., for a film thickness which is much smaller than the characteristic wetting length δ_w, which is unrealistic. Thus, one concludes that periodic arrays of wires are unstable in any practical case.

Now consider a *two-layer* wetting potential defined by Eq. (2). We expand Eq. (2) around the initial film thickness and obtain

$$w_2 = -\frac{w_1}{2}, \quad w_3 = \frac{w_1}{6}. \tag{41}$$

Thus, for $w_1=w_{1c}=1/4$, we have $\lambda \equiv 0$. In this case, system (35) fails to describe periodic patterns with a constant amplitude $A=\text{const}$, $B=0$, since there is no nonlinear saturation; the latter appears in higher orders of ε. Thus, we introduce a new slow time scale $T=\varepsilon^4 t$ and repeat the multiple-scale analysis described above. At $O(\varepsilon^5)$, we obtain (neglecting spatial modulations of A that decay on the faster time scale, $\varepsilon^2 t$)

$$A_T = \frac{1}{4}\sigma A - \kappa|A|^4A, \tag{42}$$

where

$$\kappa = \frac{w_1}{4(3+4w_1)} = \frac{1}{64} \tag{43}$$

at $w_1=w_{1c}$. Therefore, for the two-layer wetting model, the amplitude of one-dimensional (1D), stable periodic structures is of $O(\varepsilon^{1/4})$.

We now consider the general case of two-dimensional structures. Due to quadratic nonlinearity, a hexagonal pattern (hexagonal array of dots) will be preferable.[23,39] We take $\mathbf{X}=\varepsilon\mathbf{x}$, $\tau=\varepsilon t$ and $T=\varepsilon^2 t$, $\varepsilon << 1$, use expansions (30) and (28), and consider

$$H_1 = \sum_{n=1}^{3} A_n(\mathbf{X},T)e^{i\mathbf{k}_n\cdot\mathbf{x}}, \tag{44}$$

$$H_2 = B(\mathbf{X},T) + \sum_{n=1}^{3} C_n(\mathbf{X},T)e^{2i\mathbf{k}_n\cdot\mathbf{x}} + D_1(\mathbf{X},T)e^{i(\mathbf{k}_1-\mathbf{k}_2)\cdot\mathbf{x}} + D_2(\mathbf{X},T)e^{i(\mathbf{k}_1-\mathbf{k}_3)\cdot\mathbf{x}} + D_3(\mathbf{X},T)e^{i(\mathbf{k}_2-\mathbf{k}_3)\cdot\mathbf{x}} + \text{c.c.} + \cdots, \tag{45}$$

where $\mathbf{k}_1+\mathbf{k}_2+\mathbf{k}_3=0$, $|\mathbf{k}_{1,2,3}|=k_c$. The linear operator $\mathcal{E}_1$ acting on a Fourier harmonic $A(\mathbf{X},T)e^{i\mathbf{k}\cdot\mathbf{x}}$ is expanded similar to Eq. (33) as

$$\mathcal{E}_{10}(\mathbf{k}) = -|\mathbf{k}|, \quad \mathcal{E}_{11}(\mathbf{k},\boldsymbol{\nabla}) = \frac{i}{|\mathbf{k}|}\mathbf{k}\cdot\boldsymbol{\nabla},$$

$$\mathcal{E}_{12}(\mathbf{k},\boldsymbol{\nabla}) = \frac{1}{2|\mathbf{k}|}\left(\nabla^2 - \frac{1}{|\mathbf{k}|^2}(\mathbf{k}\cdot\boldsymbol{\nabla})^2\right), \tag{46}$$

and $\boldsymbol{\nabla}$ acts on the long-scale coordinates $\mathbf{X}$. We substitute these expansions into Eq. (23) and obtain the following set of amplitude equations at third and fourth orders of ε:

$$\frac{\partial A_1}{\partial T} = \frac{1}{4}\sigma A_1 + (\mathbf{k}_1\cdot\boldsymbol{\nabla})^2 A_1 - \frac{1}{2}w_2 A_2^* A_3^* + 4iw_2\mathbf{k}_1\cdot\boldsymbol{\nabla}(A_2^* A_3^*) - \lambda_1|A_1|^2 A_1 - \lambda_2(|A_2|^2+|A_3|^2)A_1 + sA_1 B, \tag{47}$$

$$\frac{\partial B}{\partial T} = \frac{1}{4}\nabla^2 B - 4s\nabla^2(|A_1|^2+|A_2|^2+|A_3|^2), \tag{48}$$

where

$$s = -\frac{1}{2}w_2, \quad \lambda_1 = \frac{3}{4}w_3 - 2w_2^2, \quad \lambda_2 = \frac{3}{2}w_3 - \frac{2w_2^2}{2-\sqrt{3}}, \tag{49}$$

and equations for A_2 and A_3 are obtained by cyclic permutation of the indices in Eq. (47).

The solution of the system (47) corresponding to a spatially periodic, hexagonal array of dots is

$$A = \frac{-w_2/2 - \text{sgn}(w_2)\sqrt{w_2^2/4 + \sigma(\lambda_1+2\lambda_2)}}{2(\lambda_1+2\lambda_2)}, \quad B = 0. \tag{50}$$

Note that for $w_2<0$ it describes the array of dots whereas for $w_2>0$ it describes the array of pits. For both the two-layer and glued-layer wetting models $w_2<0$. The solution (50) is stable for [40]

$$\lambda_1 + 2\lambda_2 > 0, \quad w_2^2 < \frac{1}{8}(\lambda_1+\lambda_2). \tag{51}$$

The first inequality in (51) ensures that the hexagonal pattern results from the transcritical bifurcation, and the second condition follows from the interaction with the zero mode that effectively renormalizes the Landau constants. It is easy to see that for the computed values of the Landau coefficients $\lambda_{1,2}$, the system (51) reduces to the first condition $\lambda_1+2\lambda_2>0$, or

$$w_3 > \frac{8}{9}\left(5 + \frac{1}{2-\sqrt{3}}\right)w_2^2 \approx 7.76w_2^2. \tag{52}$$

Thus, one can see that the necessary condition for the existence of stable hexagonal arrays of dots is $w_3>0$—i.e., $\partial^3\mathcal{W}/\partial h^3>0$. For the *two-layer* wetting potential defined by Eq. (2), $w_1=1/4$, $w_2=-1/8$, and $w_3=1/24$ and the condition (52) is not satisfied: the hexagonal array of dots results from a subcritical bifurcation and is therefore unstable. For a glued-layer wetting model defined by Eq. (4) one can check that the condition (52) can be satisfied only for $\xi \ll 1$, which is unrealistic. Thus, neither for a two-layer wetting model nor for a glued-layer can one expect the formation of stable, spatially periodic hexagonal array of dots. This can explain the fact that the formation of such arrays has never been observed in experiments. However, for some other types of wetting potentials the condition (52) might be fulfilled and in this case the self-assembly of stable, hexagonally ordered arrays of QDs would be possible. It is instructive, therefore, to rewrite (52) in terms of original physical parameters; it reads

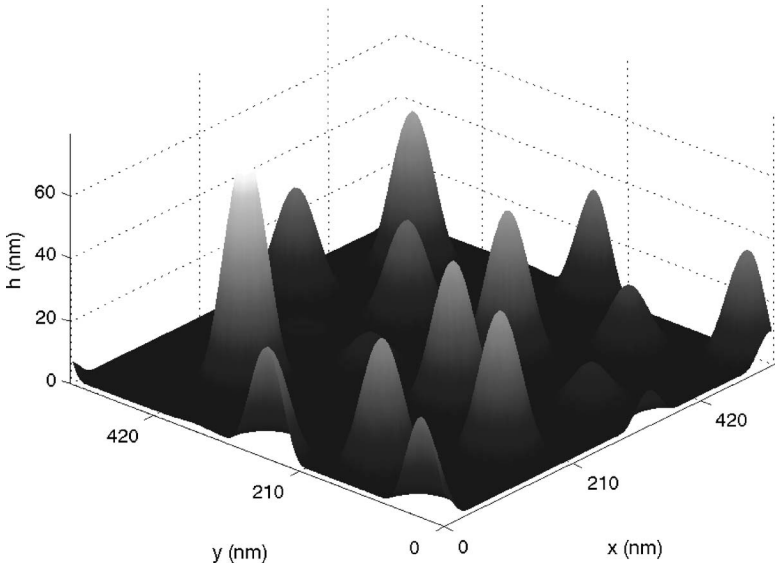

FIG. 7. Localized QDs: numerical solution of Eq. (26) with a glued-layer wetting potential at a particular moment of time for a film with initial thickness $h_0=5$ nm, $\delta_w=2$ nm, $\alpha=2$, and $\epsilon=0.025$. Other parameters are (cgs units) $\mu_0=0.8$, $w=10^8$, $\nu_f=0.198$, and $\nu_s=0.217$.

$$\epsilon^4 \frac{\mu_f^2}{\gamma_f}\left(\frac{\mu_f}{\mu_s}\right)^2\left(\frac{1+\nu_f}{1-\nu_f}\right)^4(1-\nu_s)^2\frac{\partial^3 \mathcal{W}/\partial h^3}{(\partial^2 \mathcal{W}/\partial h^2)^2} > \frac{1}{12}\left(5+\frac{1}{2-\sqrt{3}}\right) \approx 0.73. \quad (53)$$

Also recall that for $\partial^2 \mathcal{W}/\partial h^2 < 0$ one expects the formation of an array of dots whereas for $\partial^2 \mathcal{W}/\partial h^2 > 0$ a hexagonal array of pits will form instead.

VII. NUMERICAL SIMULATIONS

We have performed numerical simulations of Eq. (26) for the glued-layer wetting potential, $W(H)=\bar{w}H^{-\alpha_w}e^{-H}$, by means of a pseudospectral method with the time integration in Fourier space using the Crank-Nicolson scheme for the linear operator and the Adams-Bashforth scheme for the nonlinear operator. The simulations support the main conclusion of the weakly nonlinear analysis, that near the instability threshold, the stationary, spatially periodic structures are unstable as a result of a subcritical bifurcation for $H_0 > 1$. Figure 7 shows the solution of Eq. (26) at a particular moment in time in a relatively small domain, for small supercriticality. One can see the formation of spatially localized islands. We have found that this system of islands coarsens in time, with larger islands growing at the expense of the smaller ones.

The formation and evolution of surface structures in a large domain is shown in Fig. 8 along with the corresponding Fourier spectra. In Fig. 8(a), one can see the formation of the surface structure characterized by the preferred wavelength determined by the linear stability analysis: the Fourier spectrum is a well-defined ring corresponding to the most rapidly growing mode in the narrow interval of unstable modes near k_c. Note that there is no hexagonal ordering in this structure. At later stages [Figs. 8(b)–8(d)] the structure exhibits coarsening in that some dots grow in height at the expense of smaller dots and the average distance between the dots increases. Thus, the system of spatially localized dots forms, with the average distance between the dots much larger than the localization region (dot width). This is also seen in the corresponding Fourier spectra in Figs. 8(c) and 8(d). It is interesting to note that the width of the islands remains almost constant as the structure coarsens. This can be seen in Fig. 9. The mass from the shrinking islands is redistributed into the heights of the growing islands without contributing to their widths.

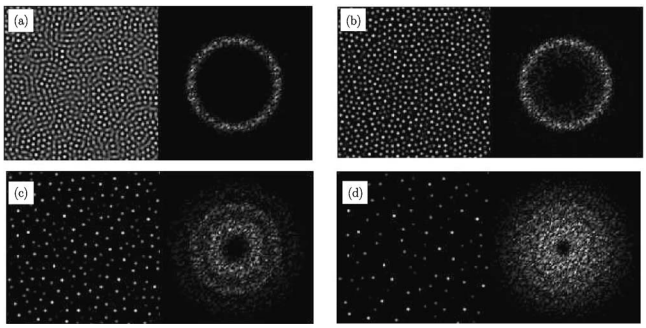

FIG. 8. Solutions of Eq. (26) in real and Fourier space for dimensionless times (a) $t=200$, (b) $t=250$, (c) $t=350$, and (d) $t=450$. The parameters are the same as in Fig. 7.

The coarsening kinetics of QDs can be characterized by different parameters. Figure 10(a) shows the time dependence of the "root-mean-square" surface roughness $\langle r \rangle$ suggested in Ref. 29 defined as $\langle r \rangle = N^{-1}(\Sigma_{m,n=1,N}[h_{m,n}-h_0]^2)^{1/2}$, where $h_{m,n}$ is the value of h at a discrete point (m,n), $N=512^2$ is the total number of points, h_0 is the initial film thickness (equal to the mean value $\langle h \rangle$ due to conservation of mass), and the result is averaged over ten realizations corresponding to ten different random initial data. One can see that $\langle r \rangle \sim t^{\beta_1}$ where $\beta_1 \approx 2.88$. Figure 10(b) presents the time dependence of the maximum height of the surface structures, $\langle h_{max} \rangle$, averaged over the realizations. Here, one can see that at the late stages of coarsening $\langle h_{max} \rangle(t)$ exhibits the power-law increase, $\langle h_{max} \rangle \sim t^{\beta_2}$,where $\beta_2 \approx 4.23$. Figure 10(c) shows the average distance between the dots, $\langle d \rangle$, as a function of time. Here, $\langle d \rangle$ is computed as $\langle d \rangle = (N/N_+)^{1/2}$, where N_+ is the number of points for which $h-h_0>0$. One can see that $\langle d \rangle \sim t^{\beta_3}$, where $\beta_3 \approx 1.45$. Thus, $\beta_1 \approx 2\beta_3$ and $\beta_2 \approx 3\beta_3$. The origin of the coarsening exponents β_1, β_2, and β_3 and relation between them is yet to be understood.

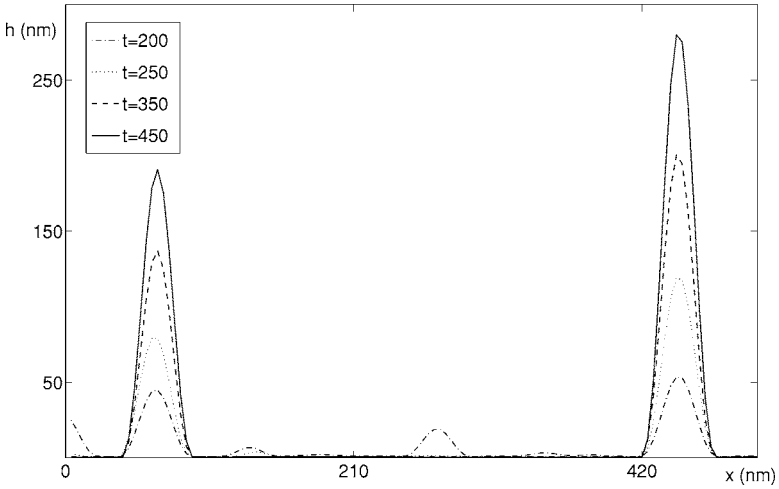

FIG. 9. Coarsening of QDs: x cross section of a numerical solution of Eq. (26) at different moments of time. Parameters are the same as in Fig. 7.

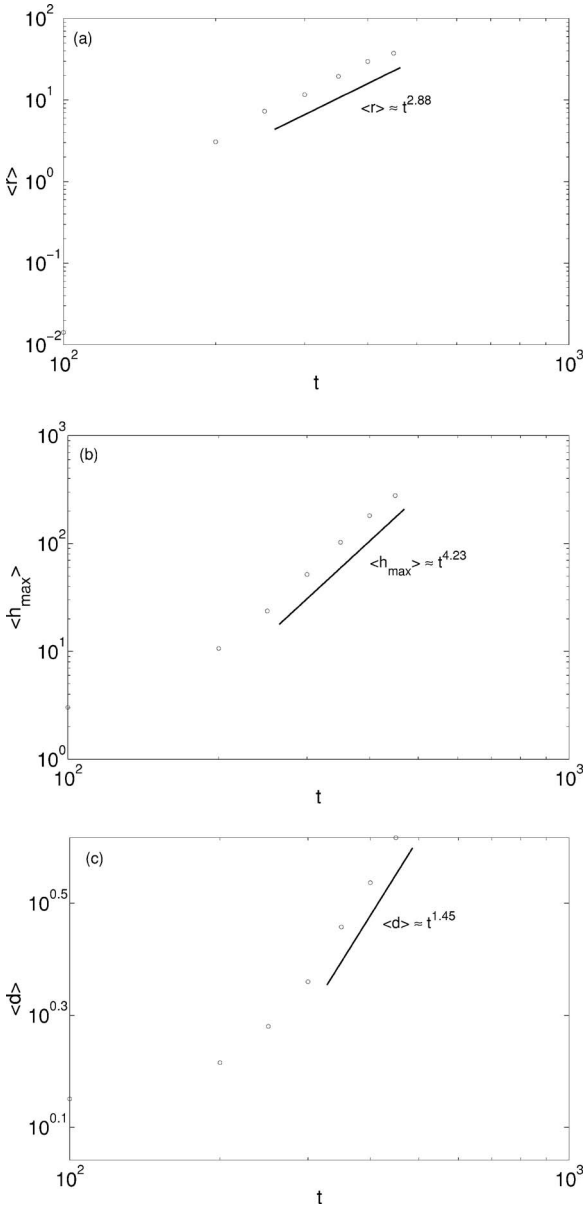

FIG. 10. Time dependence of (a) root-mean-square surface roughness, (b) maximum height of surface structures, and (c) average distance between dots.

VIII. CONCLUSIONS

We have studied the evolution of the Asaro-Tiller-Grinfeld instability of an epitaxially strained thin solid film on a solid substrate in the case when the film wets the substrate. We have shown that generally, in the presence of wetting interactions, the stress-balance-boundary conditions of the corresponding elasticity problem must include an additional term that describes the *wetting stress* resulting from the dependence of the wetting potential on the film thickness change caused by elastic deformation. We have shown that the wetting stress breaks the symmetry between the tensile and compressive epitaxial strains in that the elastically stressed state of the planar film and its stability boundaries depend on the different models of epitaxial strain. Wetting strain is a minor effect for typical semiconductor systems, such as Ge on Si; however, it may be important for hard solid films on relatively soft substrates.

We have derived a nonlocal, integro-differential equation describing the evolution of the film shape in the long-wave approximation in the general case with the wetting stress. When the latter can be neglected (for a typical semiconductor system) we have performed a weakly nonlinear analysis near the instability threshold and have found general conditions on the wetting potential for which self-assembly of spatially regular arrays of QDs can be observed. We have shown that these conditions are not met in the case of a two-layer and glued-layer wetting potentials and, therefore, spatially regular QD arrays are unstable in these cases. This can explain the fact that the spontaneous formation of spatially regular QD arrays has not been observed in experiments in semiconductors.

We have performed numerical simulations of the derived evolution equation and investigated the formation and evolution of QDs in large domains. We have found that after the structure with the wavelength corresponding to the most rapidly growing mode is formed, the system exhibits coarsening, with large islands growing at the expense of the smaller ones. We have also observed that during the coarsening the width of the localized dots remains almost unchanged while the height grows. We have found that the coarsening rate obeys power laws, with different characteristics, such as root-mean-square roughness, maximum dot height, and average distance between the dots having different coarsening exponents: $\beta_1 = 2.88$, $\beta_2 = 4.23$, and $\beta_3 = 1.45$, respectively.

ACKNOWLEDGMENT

This work was supported by National Science Foundation Grant No. DMR-0102794.

[1] V. A. Shchukin and D. Bimberg, Rev. Mod. Phys. **71**, 1125 (1999).
[2] D. Bimberg, M. Grundmann, and N. N. Ledentsov, *Quantum Dot Heterostructures* (Wiley, Chichester 1999).
[3] J. Stangl, V. Holy, and G. Bauer, Rev. Mod. Phys. **76**, 725 (2004).
[4] D. J. Mowbray and M. S. Skolnik, J. Phys. D **38**, 2059 (2005).
[5] J. M. Klostranec and W. C. W. Chan, Adv. Mater. (Weinheim, Ger.) **18**, 1953 (2006).
[6] R. J. Asaro and W. A. Tiller, Metall. Trans. **3**, 1789 (1972); M. Y. Grinfeld, Sov. Phys. Dokl. **31**, 831 (1986).
[7] D. J. Srolovitz, Acta Metall. **37**, 621 (1989).

[8] B. J. Spencer, P. W. Voorhees, and S. H. Davis, Phys. Rev. Lett. **67**, 3696 (1991).
[9] B. J. Spencer, S. H. Davis, and P. W. Voorhees, Phys. Rev. B **47**, 9760 (1993).
[10] B. J. Spencer, P. W. Voorhees, and S. H. Davis, J. Appl. Phys. **73**, 4955 (1993).
[11] F. M. Ross, J. Tersoff, and R. M. Tromp, Phys. Rev. Lett. **80**, 984 (1998).
[12] J. A. Floro, M. B. Sinclair, E. Chason, L. B. Freund, R. D. Twesten, R. Q. Hwang, and G. A. Lucadamo, Phys. Rev. Lett. **84**, 701 (2000).
[13] K. Alchalabi, D. Zimin, G. Kostorz, and H. Zogg, Phys. Rev. Lett. **90**, 026104 (2003).
[14] G. Springholz, V. Holy, M. Pinczolits, and G. Bauer, Science **282**, 734 (1998); M. Pinczolits, G. Springholz, and G. Bauer, Phys. Rev. B **60**, 11524 (1999).
[15] Y. W. Zhang, Phys. Rev. B **61**, 10388 (2000); Y. W. Zhang and A. F. Bower, Appl. Phys. Lett. **78**, 2706 (2001); P. Liu, Y. W. Zhang, and C. Lu, Phys. Rev. B **68**, 035402 (2003).
[16] V. A. Shchukin, D. Bimberg, T. P. Munt, and D. E. Jesson, Ann. Phys. (N.Y.) **320**, 237 (2005).
[17] V. Holy, G. Springholz, M. Pinczolits, and G. Bauer, Phys. Rev. Lett. **83**, 356 (1999).
[18] G. Springholz, C. R. Phys. **6**, 89 (2005).
[19] P. Liu, Y. W. Zhang, and C. Lu, Phys. Rev. B **68**, 195314 (2003).
[20] H. R. Eisenberg and D. Kandel, Phys. Rev. Lett. **85**, 1286 (2000); Phys. Rev. B **66**, 155429 (2002).
[21] A. A. Golovin, S. H. Davis, and P. W. Voorhees, Phys. Rev. E **68**, 056203 (2003).
[22] T. V. Savina, P. W. Voorhees, and S. H. Davis, J. Appl. Phys. **96**, 3127 (2004).
[23] D. Walgraef, *Spatio-Temporal Pattern Formation* (Springer, New York, 1997).
[24] A. A. Golovin, M. S. Levine, T. V. Savina, and S. H. Davis, Phys. Rev. B **70**, 235342 (2004).
[25] C.-H. Chiu, Phys. Rev. B **69**, 165413 (2004).
[26] H. R. Eisenberg and D. Kandel, Phys. Rev. B **71**, 115423 (2005).
[27] W. T. Tekalign and B. J. Spencer, J. Appl. Phys. **96**, 5505 (2004).
[28] Y. Xiang and E. Weinan, J. Appl. Phys. **91**, 9414 (2002).
[29] Y. Pang and R. Huang, Phys. Rev. B **74**, 075413 (2006).
[30] S. M. Wise, J. S. Lowengrub, J. S. Kim, K. Thornton, P. W. Voorhees, and W. C. Johnson, Appl. Phys. Lett. **87**, 133102 (2005).
[31] D. J. Seol, S. Y. Hu, Z. K. Liu, L. Q. Chen, S. G. Kim, and K. H. Oh, J. Appl. Phys. **98**, 044910 (2005).
[32] L. D. Landau and E. M. Lilfshits, *Elasticity Theory* (Pergamon Press, New York, 1981).
[33] C. H. Chiu and H. Gao, in *Thin Films: Stresses and Mechanical Properties V*, edited by S. P. Baker, MRS Symposia Proceedings No. 356 (Materials Research Society, Pittsburgh, 1995), p. 33.
[34] J. Tersoff, Phys. Rev. B **43**, 9377 (1991).
[35] M. J. Beck, A. van de Walle, and M. Asta, Phys. Rev. B **70**, 205337 (2004).
[36] M. Ortiz, E. A. Repetto, and H. Si, J. Mech. Phys. Solids **47**, 697 (1999).
[37] Z. Suo and Z. Zhang, Phys. Rev. B **58**, 5116 (1998).
[38] B. J. Spencer, Phys. Rev. B **59**, 2011 (1999).
[39] M. C. Cross and P. C. Hohenberg, Rev. Mod. Phys. **65**, 851 (1993).
[40] S. M. Cox and P. C. Matthews, Physica D **175**, 196 (2003).